Supplementary material

Investigation of the Interaction Between the Atypical Agonist c[YpwFG] and MOR.

Luca Gentilucci,*[a] Federico Squassabia,[a] Rossella Demarco,[a] Roberto Artali, [b§] Giuliana Cardillo,[a†] Alessandra Tolomelli,[a] Santi Spampinato,[c‡] Andrea Bedini.[c]

[a] *Dipartimento di Chimica "G. Ciamician", Università degli Studi di Bologna, via Selmi 2, 40126-Bologna, Italy.* [b] *Istituto di Chimica Farmaceutica e Tossicologica "P. Pratesi", Università di Milano, Via Mangiagalli 25, 20133 - Milano.* [c] *Dipartimento di Farmacologia, Università degli Studi di Bologna, via Irnerio 42, 40126-Bologna, Italy.*

* E-mail: luca.gentilucci@unibo.it; Phone: +39 051 2099575; Fax: +39 051 2099456. [§] E-mail: roberto.artali@gmail.com; Phone: +39 02 50319308; Fax: +39 02 50317565. [†] E-mail: giuliana.cardillo@unibo.it; Phone: +39 051 2099570. [‡] E-mail: spampi@biocfarm.unibo.it; Phone: +39 051 2091851

Contents

Spectroscopic characterization[a]

***c*[YpwFG]** (**3**). ^{1}H NMR (DMSO-d_6) δ: 10.62 (s, 1H, Y-OH); 9.25 (s, 1H, w-NH_1); 8.46 (d, J= 5.6, 1H, Y-NH), 8.38 (d, J= 8.4, 1H, F-NH); 7.84 (dd, J= 1.6, 8.4, 1H, G-NH); 7.51 (d, J= 7.6, 1H, w-H_4); 7.30 (d, J= 6.8, 1H, w-NH); 7.29 (d, J= 8.0, 1H, w-H_7); 7.12-7.19 (m, 3H, F-ArH_{3-5}); 7.05-7.10 (m, 2H, F-$ArH_{2,6}$); 7.02 (t, J= 7.2, 1H, w-H_6); 6.98 (d, J= 8.0, 2H, Y-$HAr_{2,6}$), 6.92 (t, J= 7.2, 1H, w-H_5); 6.79 (s, 1H, w-H_2); 6.65 (d, J= 8.0, 2H, Y-$HAr_{3,5}$); 4.49 (q, J= 6.8, 1H, w-Hα); 4.42 (q, J= 8.0, 1H, F-Hα); 4.36 (dt, J= 5.6, 8.0, 1H, Y-Hα); 4.27 (dd, J= 8.4, 14.8, 1H, G-Hα); 4.07 (dd, J= 3.6, 8.0, 1H, p-Hα); 3.55-3.65 (m, 1H, p-$H\delta_{down}$); 3.15 (dd, J= 1.6, 14.8, 1H, G-Hα); 3.13 (dd, J= 9.1, 14.4, 1H, w-Hβ); 2.96 (dd, J= 6.8, 14.0, 1H, F-Hβ); 2.79 (dd, J= 5.2, 14.4, 1H, w-Hβ); 2.74 (d, J= 8.0, 2H, Y-Hβ); 2.68-2.78 (m, 1H, p-$H\delta_{up}$); 2.66 (dd, J= 8.0, 14.0, 1H, F-Hβ); 1.75-1.86 (m, 1H, p-$H\beta_{up}$); 1.55-1.68 (m, 2H, p-$H\beta_{down}$ + p-$H\gamma_{down}$); 1.46-1.55 (m, 1H, p-$H\gamma_{up}$).

***c*[YpwFp]** (**7**).[b] ^{1}H NMR (DMSO-d_6) δ: 10.71 (s, 1H, w-NH_1); 9.27 (s, 1H, Y-OH); 8.13 (d, J= 7.6, 1H, Y-NH); 7.86 (d, J= 8.8, 1H, F-NH); 7.67 (d, J=8.0, w-NH); 7.45 (d, J= 8.0, w-H_4); 7.29 (d, J= 8.0, 1H, w-H_7); 7.14-7.26 (m, 5H, F-ArH); 7.03 (t, J= 7.2, 1H, w-H_6); 6.95 (d, J= 8.4, 2H, Y-$ArH_{2,6}$); 6.92 (s, 2H, w-H_2+w-H_5); 6.66 (d, J= 8.4, 2H, Y-$ArH_{3,5}$); 4.74 (q, J= 7.2, 1H, F-Hα); 4.64 (d, J= 7.2, 1H, p^5-Hα); 4.54 (q, J= 7.6, 1H, Y-Hα); 4.39 (q, J= 6.4, 1H, w-Hα); 3.97 (dd, J= 8.0, 6.0, 1H, p^2-Hα); 3.45-3.55 (m, 1H, p^2-$H\delta_{down}$); 3.36-3.45 (m, 1H, p^5-$H\delta_{down}$); 3.26 (dd, J= 14.8, 4.8, 1H, w-Hβ); 3.10-3.19 (m, 1H, p^5-$H\delta_{up}$); 3.05 (dd, J= 13.6, 8.8, 1H, F-Hβ); 2.86 (dd, J= 14.8, 8.4, 1H, w-Hβ); 2.62-2.76 (m, 5H, p^2-$H\delta_{up}$+F-Hβ+Y-Hβ); 2.05-2.13 (m, 1H, p^5-$H\beta_{down}$); 1.70-1.89 (m, 3H, p^5-$H\gamma_{up}$+ p^5-$H\gamma_{down}$+p^2-$H\beta_{up}$); 1.55-1.70 (m, 2H, p^2-$H\gamma_{down}$+p^5-$H\beta_{up}$); 1.45-1.55 (m, 1H, p^2-$H\beta_{down}$); 1.39-1.45 (m, 1H, p^2-$H\gamma_{up}$).

***c*[YpwFP]** (**8**). ^{1}H NMR (DMSO-d_6) δ: 10.75 (s, 1H, w-NH_1); 9.29 (s, 1H, Y-OH); 8.41 (d, J= 6.0, 1H, Y-NH); 7.55 (d, J= 8.0, 1H, w-H_4); 7.49 (d, J= 8.6, 1H, F-NH); 7.27 (d, J=8.0, 1H, w-H_7); 7.10-7.21 (m, 5H, F-ArH); 7.05 (d, J= 8.0, 2H, Y-$ArH_{2,6}$); 7.03 (s, 1H, w-H_2); 7.01 (t, J=7.6, 1H, w-H_6); 6.93 (t, J= 7.4, w-H_5); 6.79 (d, J= 9.6, 1H, w-NH); 6.66 (d, J= 8.0, 2H, Y-$ArH_{3,5}$); 4.46-4.59 (m, 2H, Y-Hα+F-Hα); 4.12-4.24 (m, 1H, w-Hα); 4.02 (d, J=8.8, 1H, P-Hα); 3.95-4.05 (m, 1H, p-Hα); 3.75-3.85 (m, 1H, P-$H\delta_{down}$); 3.60 (q, J= 8.8, 1H, p-$H\delta_{down}$); 3.45 (dd, J=12.8, 4.0, 1H, F-Hβ); 3.30-3.40 (m, 1H, P-$H\delta_{up}$); 3.18 (dd, J=13.6, 3.0, 1H, w-Hβ); 2.80-2.99 (m, 4H, F-Hβ+Y-Hβ+ p-$H\delta_{up}$); 2.78 (dd, J=13.6, 11.6, 1H, w-Hβ); 1.98-2.09 (m, 1H, P-$H\beta_{up}$); 1.81-1.98 (m, 1H, P-$H\beta_{down}$); 1.65-

1.80 (m, 2H, P-Hγ_{up}+p-Hβ_{up}); 1.45-1.52 (m, 2H, P-Hγ_{down}+ p-Hγ_{down}); 1.20-1.35 (m, 1H, p-Hγ_{up}); 0.60-0.78 (m, 1H, p-Hβ_{up}).

[a] br. = broad; p = D-Pro, w = D-Trp; H_{up} is defined as the proton lying on the same side as p-Hα; H_{down} is defined as the proton lying on the opposite side as p-Hα; Js are expressed in Hz.
[b] p^2 = D-Pro^2, p^5 = D-Pro^5.

Table S1. $\Delta\delta/\Delta t$ values (ppb/°K) of amide protons for **3**, **7**, **8** determined by VT-^{1}H-NMR analysis in DMSO-d_6 at 400 MHz over the range 298-348 °K

Compd	$\Delta\delta/\Delta t$ TyrNH	$\Delta\delta/\Delta t$ D-TrpNH	$\Delta\delta/\Delta t$ PheNH	$\Delta\delta/\Delta t$ GlyNH
3	-4.8	-1.5	-5.3	-1.4
7	-2.7	-2.5	-6.3	-
8	-8.3	-1.5	-0.2	-

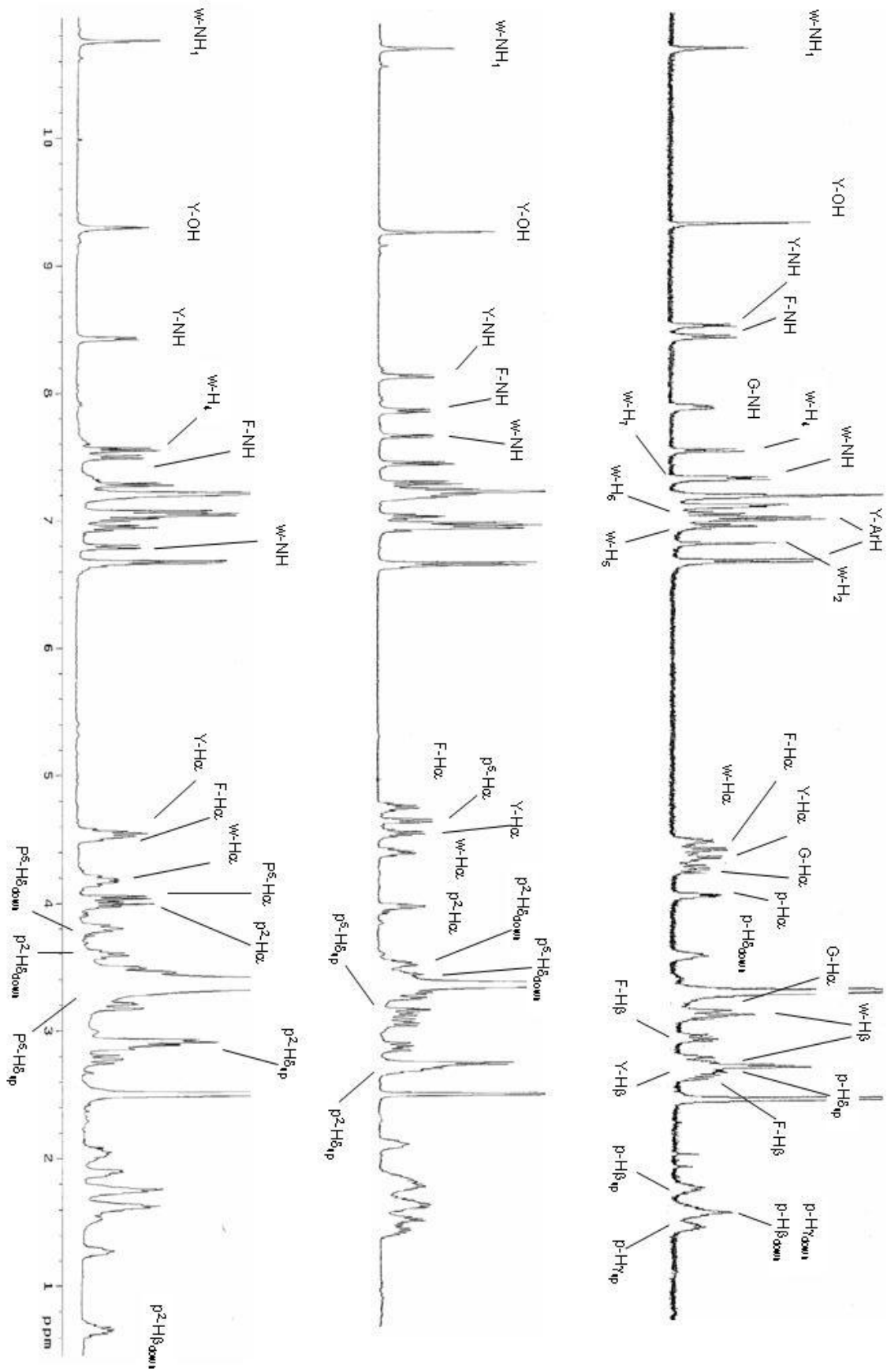

Figure S1. ^{1}H-NMRs of **3**, **7**, and **8**.

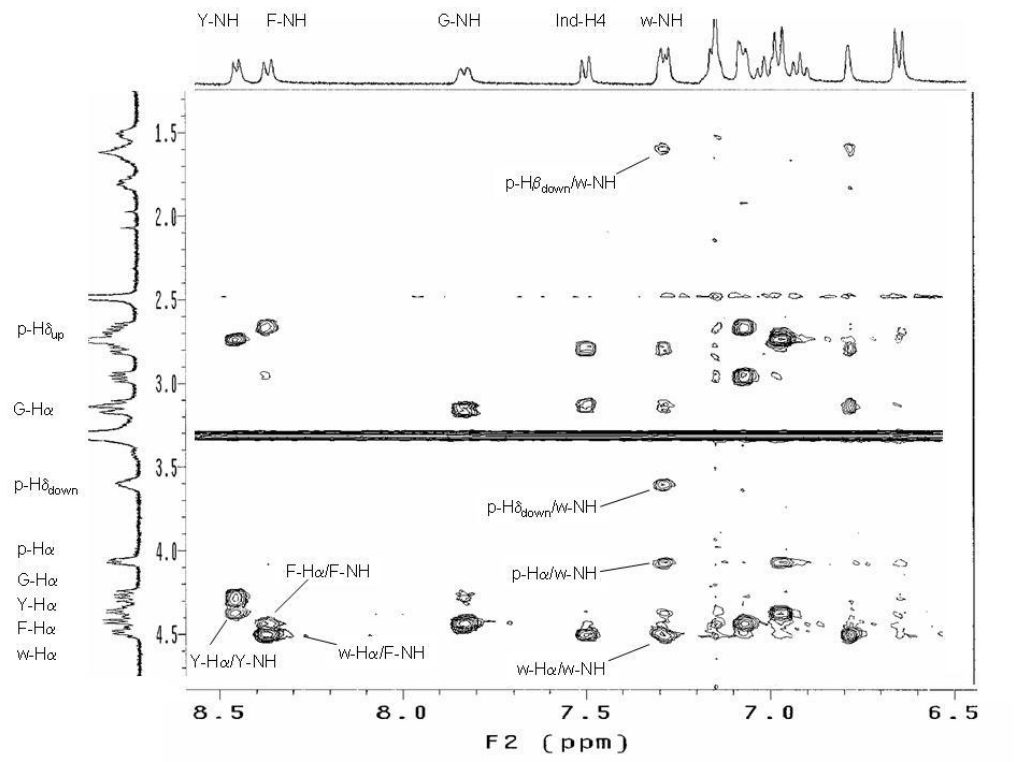

Figure S2. ROESY analysis of **3** (400 MHz, DMSO-d_6); inset of the strategic region of amide NH-Hα cross-peaks.

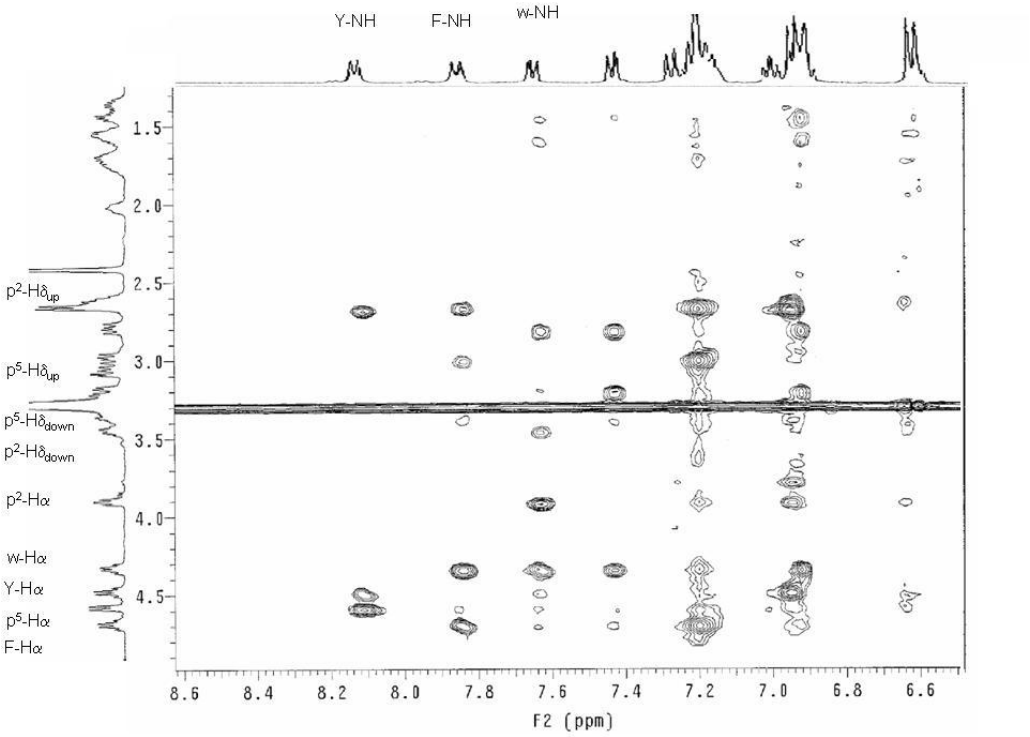

Figure S3. ROESY analysis of **7** (400 MHz, DMSO-d_6); inset of the strategic region of amide NH-Hα cross-peaks.

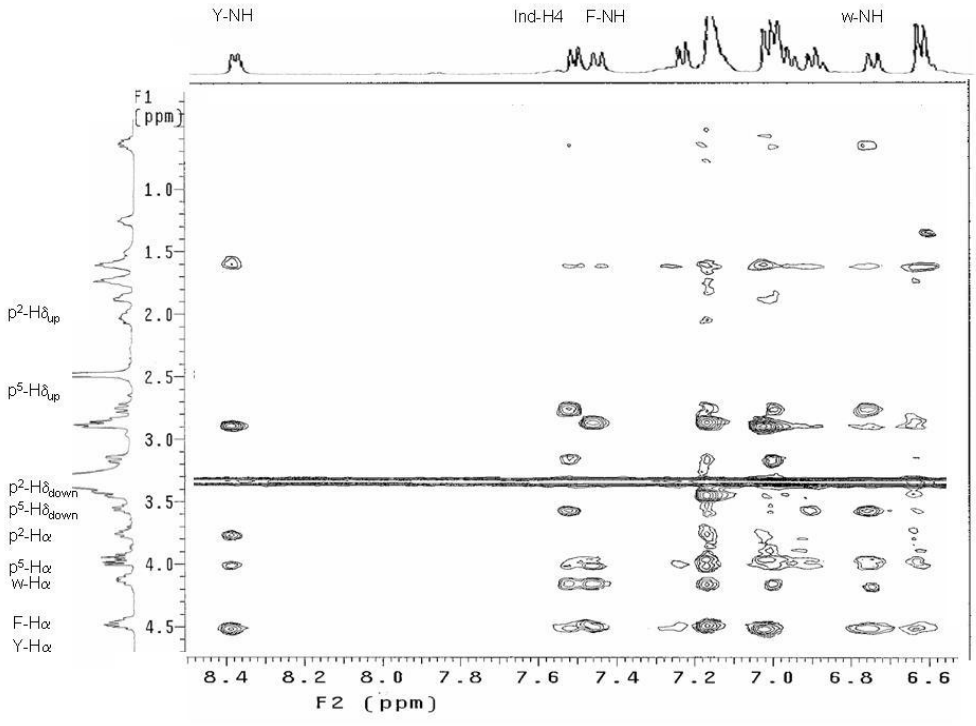

Figure S4. ROESY analysis of **8** (400 MHz, DMSO-d_6); inset of the strategic region of amide NH-Hα cross-peaks.

Table S2. Non-obvious ROESY cross-peaks observed for **3**.[a]

Cross peak	**Intensity**	**Cross peak**	**Intensity**
Y-Hα - p-Hδ_{down}	vs	w-H_2 – w-Hα	vs
p-Hγ_{down} - w-NH	w	F-NH – G-NH	w
p-Hγ_{down} - w-H_2	w	Y-NH – G-NH	w
G-NH - G-H$\alpha_{3.2}$	vs	Y-NH – F-NH	w
G-NH - G-H$\alpha_{4.3}$	m	Y-NH – Y-H$Ar_{2,6}$	m
p-Hδ_{down} - w-NH	m	F-NH – w-NH	m
p-Hα - w-NH	m	F-NH – F-H$Ar_{2,6}$	vs
p-Hα - Y-H$Ar_{2,6}$	m	F-NH – w-H_2	m
Y-NH - G-H$\alpha_{4.3}$	vs	w-Hα - w-H$\beta_{3.1}$	s
Y-NH - Y-Hα	s	w-Hα - w-H$\beta_{2.8}$	s
F-NH - F-Hα	s	F-Hα - F-H$\beta_{2.8}$	s
F-NH – w-Hα	vs	F-Hα - F-H$\beta_{3.1}$	s
G-NH - H_α	vs	w-H_4 – w-H$\beta_{2.8}$	vs
w-H_α - w-H_4	s	w-NH – w-H$\beta_{3.1}$	m
w-NH – w-Hα	s	w-NH – w-H$\beta_{2.8}$	m
Y Hα - w-NH	w	w-H$\beta_{3.1}$ – w-H_2	vs
F-Hα - F-H$Ar_{2,6}$	vs	p-Hα - Y-H$Ar_{3,4}$	w
Y-Hα - Y-H$Ar_{2,6}$	vs	w-H_2 – w-H$\beta_{2.8}$	m

Table S3. Non obvious ROESY cross-peaks observed for **7**.[a]

Cross peak	Intensity	Cross peak	Intensity
Y-NH – Y-Hα	s	Y-NH – p^5-Hα	vs
Y-NH – Y-ArH	s	Y-NH – F-NH	s
F-NH – F-H$\beta_{2.6}$	s	F-NH – F-H$\beta_{3.1}$	m
F-NH – p^5-Hδ_{down}	w	F-NH – w-Hα	vs
F-NH – F-Hα	s	F-NH – w-NH	s
w-NH – w-H_2	m	w-NH – p^2-Hβ_{down}	w
w-NH – p^2-Hγ_{down}	w	w-NH – w-H$\beta_{2.8}$	m
w-NH – w-H$\beta_{3.2}$	w	w-NH – p^2-Hδ_{down}	m
w-NH – p^2-Hα	s	w-NH – w-Hα	s
w-NH – Y-Hα	w	w-NH – p^5-Hα	w
w-NH – F-Hα	w	w-H_4 – p^2-Hβ_{down}	w
w-H_4 – w-H$\beta_{3.2}$	s	w-H_4 – w-H$\beta_{2.8}$	s
w-H_4 – w-Hα	s	w-H_4 – F-Hα	s
F-ArH – F-Hα	vs	F-ArH – F-NH	m
w-H_2 – w-Hα	vs	Y-ArH – Y-Hα	vs
F-Hα – F-H$\beta_{2.7}$	s	F-Hα – F-H$\beta_{3.0}$	m
F-Hα – p^5-Hδ_{up}	vs	F-Hα – p^5-Hδ_{down}	s
Y-Hα – p^2-Hδ_{up}	m	Y-Hα – p^2-Hδ_{down}	vs
w-Hα – w–H$\beta_{2.8}$	m	w-Hα – w–H$\beta_{3.2}$	s
w-Hα - F-ArH	m	P^2-Hδ_{up} - Y-ArH	m
p^5-Hα - F-NH	w		

Table S4. Non obvious ROESY cross-peaks observed for **8**.[a]

Cross peak	Intensity	Cross peak	Intensity
Y-NH – P-Hγ_{down}	m	Y-NH – Y-ArH	m
Y-NH – P-Hδ_{down}	s	Y-NH – F-NH	m
Y-NH – P-Hα	m	Y-NH – Y-Hα	s
w-H_4 – P-Hα	w	w-H_4 – p-Hβ_{down}	w
w-H_4 – w-H$\beta_{2.8}$	vs	w-H_4 – w-H$\beta_{3.3}$	m
w-H_4 – p-Hδ_{down}	s	w-H_4 – w-Hα	m
w-H_4 – w-NH	s	F-NH – F-H$\beta_{2.9}$	vs
F-NH – P-Hα	m	F-NH – w-Hα	s

F-NH – F-Hα	m	F-NH – w-NH	vs
F-NH - Y-Hα	m	Y-Ar$H_{2,6}$ – Y-Hα	vs
Y-Ar$H_{2,6}$ – Y-NH	s	w-H_2 – w-H$\beta_{2.8}$	m
w-H_2 – w-H$\beta_{3.2}$	s	w-H_2 – w-Hα	vs
w-H_2 – p-Hδ_{down}	w	w-H_5 – p-Hδ_{down}	m
w-NH - p-Hβ_{down}	m	w-NH - w-H$\beta_{2.8}$	vs
w-NH - p-Hδ_{down}	s	w-NH – w-Hα	s
w-NH – Y-Hα	w	w-NH - p-Hα	w
w-NH - P-Hα	w	Y-Hα - p-Hδ_{down}	m
F-Hα – P-Hα	m	F-Hα – F-ArH	vs
w-Hα- w-H$\beta_{2.8}$	w	w-Hα- w-H$\beta_{3.2}$	m
w-Hα- F-ArH	m	P-Hα- F-ArH	m
p-Hα- Y-ArH	m		

[a] vs = very strong, s = strong, m = medium, w = weak

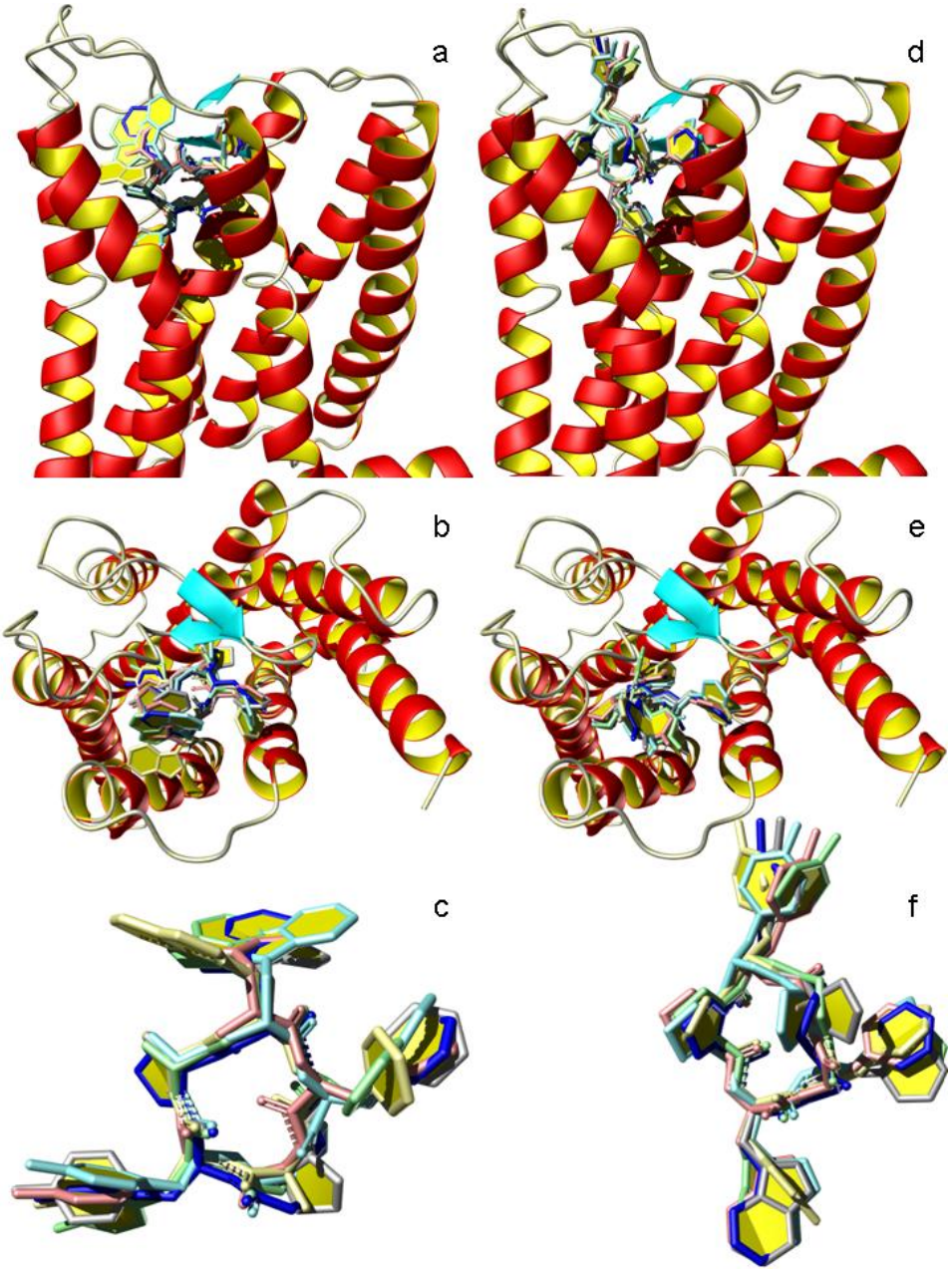

Figure S5. Side view of *Orientation 1* (a), *Orientation 2* (d), and top view of *Orientation 1* (b), *Orientation 2* (e), of cyclopeptides **3-8** docked into the binding site of MOR using AutoDock, and details of the superimposed structures of **3-8** in *Orientation 1* (c), *Orientation 2* (f). The cyclopeptides have been rendered in stick; the MOR is show by the cartoon representation and coloured by secondary structure succession. All the figures were prepared using PyMol.

Table S5. Residue within 5 Å of **3** in the two orientations identified by AutoDock.

		Orientation				Orientation	
TMH/EL	Residue	1	2	TMH/EL	Residue	1	2
TMH III	Asp147	+	*	TMH V	Asn230	-	+
	Tyr148	-	+		Lys233	+	*
	Met151	-	*		Val326	+	-
	Phe152	-	*		Phe237	*	+
EL-2	Gly213	*	-		Ala240	+	-
	Ser214	+	-		Phe241	+	-
	Asp216	+	+	TMH VI	Trp293	*	-
	Cys217	+	-		Ile296	+	-
	Thr218	*	+		His297	+	-
	Leu219	+	+		Val300	*	+
	Thr220	-	*		Lys303	+	+
	Phe221	*	*		Ala304	-	+
	His223	+	+		Thr307	-	+
				EL-3	Glu310	-	+
				TMH VII	Thr315	+	+
					Trp318	*	*
					His319	+	+
					Ile322	+	+

*) residue at a distance ≤3Å from **3**
+) residue at a distance ≤5Å from **3**
-) residue at a distance ≥5Å from **3**

Table S6. Geometric characteristics of the MOR binding site residues within 3.5A of the cyclopeptide **3** (Orientation 1 and 2) after the QM/MM optimization.

Orientation 1				*Orientation 2*			
	Contact ($Å^2$)	*Exposed ($Å^2$)*	*%*		*Contact ($Å^2$)*	*Exposed ($Å^2$)*	*%*
Binding Site	597,375427	769,406555	78	Binding Site	537,49968	780,206726	69
W318	49,100136	148,556046	33	W318	62,831818	119,088234	53
F237	48,221581	118,398483	41	T218	36,782269	91,974495	40
T218	46,296394	79,319122	58	I322	35,52417	125,676758	28
I322	41,536057	120,740158	34	F221	34,154587	147,222824	23
D216	30,838886	72,021126	43	K303	31,823547	93,484138	34
K303	30,79351	136,542908	23	L219	30,492432	119,187988	26
F221	27,897736	121,694916	23	Y148	29,027008	149,43512	19
Y148	27,283768	116,21315	23	K233	23,601128	117,792969	20
K233	27,033585	138,730957	19	W293	22,90538	193,670059	12
W293	22,334961	169,342087	13	H223	22,711929	153,636505	15
I296	21,369629	89,759315	24	F313	21,343353	182,748825	12
L219	20,726433	110,850227	19	E229	20,905167	121,838257	17
V300	20,688656	57,401249	36	F237	20,372002	136,677841	15
D147	20,522552	95,386551	22	F152	15,336395	142,52179	11
F152	16,294098	136,868927	12	T307	13,05822	83,535149	16
H319	11,449493	112,630386	10	D147	12,494095	109,225677	11
H223	11,212189	149,913559	7	E310	11,489334	183,046722	6
T315	10,967773	120,314552	9	D216	10,622086	104,533928	10
E229	9,275925	136,29454	7	V300	10,050377	78,048927	13
C217	7,611015	71,560684	11	M151	8,836594	141,35675	6
A240	6,01701	66,78334	9	T315	8,530991	105,678108	8
V236	5,036133	124,534134	4	H319	6,705956	102,350067	7
Y299	4,975891	158,374725	3	T220	5,470413	95,115547	6
G213	4,711624	49,633621	9	A304	4,095413	65,313927	6
F241	3,465363	150,965729	2	Y299	4,013855	159,655762	3
T220	3,329819	83,822678	4	N230	2,990845	111,816444	3
M151	3,033722	139,40593	2	I296	0,945099	103,584831	1

Table S7. Geometric characteristics of the MOR binding site residues within 3.5A of the cyclopeptide **4** (Orientation 1 and 2) after the QM/MM optimization.

Orientation 1				*Orientation 2*			
	Contact ($Å^2$)	*Exposed ($Å^2$)*	*%*		*Contact ($Å^2$)*	*Exposed ($Å^2$)*	*%*
Binding Site	601,132248	788,125549	76	Binding Site	483,116425	803,377014	60
W318	54,217255	149,951599	36	W318	51,741646	122,105545	42
I322	47,784161	85,143417	56	T218	38,767776	101,033257	38
T218	45,655735	103,769386	44	K303	32,011139	97,254211	33
Y148	41,373192	136,914413	30	I322	22,008461	94,076546	23
K233	36,887375	126,352783	29	L219	21,36525	110,649345	19
K303	36,665039	170,599594	21	F313	21,268921	178,172699	12
F237	35,384071	128,324066	28	K233	21,085243	111,339867	19
W293	26,558792	198,747253	13	F237	21,015175	134,118164	16
V300	26,367413	83,032982	32	H223	20,651718	137,605621	15
D216	18,752197	119,866745	16	W293	18,814346	191,312225	10
A240	15,05386	55,428356	27	D216	17,6828	97,6521	18
L219	14,753967	103,26149	14	F221	17,304871	166,309662	10
D147	14,024246	88,783081	16	F152	16,29567	114,440536	14
T307	11,595276	112,680687	10	Y148	13,205078	157,650375	8
H223	11,351456	156,098648	7	E229	12,605743	115,72451	11
I296	11,314865	91,413864	12	T307	10,656456	84,977821	13
C217	9,824417	89,993187	11	H319	10,365211	85,286339	12
M151	7,543259	135,757843	6	V300	8,111176	81,648659	10
H319	6,971375	92,43158	8	D147	7,135323	100,632263	7
F152	6,930702	112,389854	6	T315	6,396667	113,904449	6
V236	6,891296	102,446861	7	E310	5,781067	165,331985	3
Y299	6,233536	165,159653	4	T220	4,994728	89,027084	6
E229	5,470413	109,935379	5	A304	2,205223	62,318581	4
F221	5,355545	185,087753	3	Y299	2,134323	163,519043	1
I198	3,124054	137,228409	2	I296	1,575165	104,219276	2
T315	2,997833	76,648529	4	M151	0,945099	139,164658	1
I144	0,630066	140,382736	0				

Table S8. Geometric characteristics of the MOR binding site residues within 3.5A of the cyclopeptide **5** (Orientation 1 and 2) after the QM/MM optimization.

Orientation 1				*Orientation 2*			
	Contact (Å^2)	*Exposed (Å^2)*	*%*		*Contact (Å^2)*	*Exposed (Å^2)*	*%*
Binding Site	606,523773	795,842957	76	Binding Site	479,801544	773,995544	62
I322	54,723595	131,669785	42	W318	58,399481	89,568459	65
T218	45,677782	75,743378	60	F221	47,567993	158,493881	30
W318	44,764977	168,981766	26	T218	42,749561	88,866585	48
F237	41,610275	114,449532	36	I322	34,876595	123,471542	28
K303	34,774765	145,799088	24	K233	30,257584	105,803078	29
D216	31,742073	96,322945	33	K303	29,098663	128,312027	23
K233	26,136612	148,869186	18	F237	25,42128	122,669037	21
F221	26,064445	143,169739	18	V300	21,896721	99,153015	22
V300	24,533096	78,42511	31	W293	20,664948	154,667816	13
Y148	24,424683	113,285378	22	I296	19,160042	112,363091	17
W293	23,662201	174,501694	14	E310	14,701813	209,826614	7
F152	21,929642	127,044022	17	D216	11,712799	103,049088	11
D147	21,920223	72,744858	30	F313	11,288605	194,645599	6
T315	17,39843	124,622704	14	T315	9,945488	101,565063	10
C217	16,98671	67,032379	25	L219	8,816513	90,568604	10
L219	16,9767	95,309769	18	T307	8,378403	101,578407	8
I296	16,652924	102,887489	16	T220	7,373169	95,561104	8
M151	14,438927	140,069199	10	H319	7,336021	101,824203	7
H223	13,51207	181,578476	7	Y299	6,940796	144,632996	5
H319	11,670387	124,337608	9	M151	6,490318	125,617935	5
A240	9,473602	71,889801	13	A304	5,355537	86,558205	6
V236	9,096519	107,502396	8	H223	4,801384	115,016212	4
Y299	5,37439	177,860321	3	E229	3,567665	96,158112	4
G213	4,41045	50,578716	9	F152	0,945099	128,57338	1
S214	3,900818	114,872498	3				
I144	3,465347	105,145668	3				
T307	3,169159	108,970619	3				

Table S9. Geometric characteristics of the MOR binding site residues within 3.5A of the cyclopeptide **6** (Orientation 1 and 2) after the QM/MM optimization.

Orientation 1				*Orientation 2*			
	Contact (Å^2)	*Exposed (Å^2)*	*%*		*Contact (Å^2)*	*Exposed (Å^2)*	*%*
Binding Site	646,428497	800,429626	81	Binding Site	572,920944	795,234375	72
W318	52,759285	137,665131	38	F221	50,012756	185,858932	27
I322	51,590797	88,38652	58	W318	48,412556	89,431015	54
F237	48,221573	126,68325	38	K303	46,435646	124,395996	37
T218	44,838051	83,550819	54	T218	40,076317	98,97686	40
Y148	31,854843	122,408348	26	H223	36,973236	98,063881	38
K303	30,440567	94,443924	32	I322	36,163002	108,189751	33
V300	27,093506	50,02459	54	Y148	26,471771	162,615143	16
K233	22,962311	121,716721	19	L219	24,200546	112,77285	21
W293	19,61058	174,128296	11	K233	21,391525	126,186035	17
D147	18,776764	74,55101	25	I296	18,556244	89,940285	21
D216	18,201225	117,914383	15	D147	17,983444	100,128967	18
Y299	15,57856	132,821121	12	V300	16,830509	80,785126	21
I296	14,11953	81,823174	17	E310	16,064819	211,13765	8
C217	14,032806	88,372948	16	F237	15,419052	182,014404	8
L219	12,855011	113,17083	11	D216	14,121895	101,431946	14
F152	10,907898	100,230835	11	M151	12,291214	142,079468	9
H319	7,59269	94,443001	8	E229	11,503891	101,388199	11
V236	5,031754	96,191895	5	W293	10,606003	210,131104	5
A240	4,667133	53,801075	9	T315	9,941116	103,834366	10
A304	4,095413	48,918259	8	T220	7,135323	96,444771	7
T315	3,477905	85,976639	4	F313	6,585022	193,630463	3
I144	2,835297	114,953827	2	H319	6,39093	102,551712	6
M151	2,830917	140,712402	2	A304	3,78038	71,444122	5
T307	0,237839	105,909019	0	T307	3,509895	89,692505	4
				Y299	2,693466	151,233368	2
				G213	0,630066	92,42791	1

Table S10. Geometric characteristics of the MOR binding site residues within 3.5A of the cyclopeptide **7** (Orientation 1 and 2) after the QM/MM optimization.

Orientation 1				*Orientation 2*			
	Contact (Å^2)	*Exposed (Å^2)*	*%*		*Contact (Å^2)*	*Exposed (Å^2)*	*%*
Binding Site	594,902542	787,081543	76	Binding Site	519,502838	800,436462	65
W318	57,499466	110,457626	52	W318	57,637497	138,334244	42
F237	48,803482	121,975288	40	T218	38,631126	98,58136	39
T218	45,567852	74,050758	62	H223	38,39386	136,712311	28
F221	37,042435	144,188614	26	K303	35,504677	118,487411	30
W293	32,749985	194,21463	17	I322	34,596603	150,563156	23
I322	31,778824	122,112244	26	K233	22,966675	120,633682	19
K303	31,065712	142,311707	22	D216	20,764694	93,670486	22
I296	25,762573	115,462036	22	F237	20,39389	153,531937	13
D147	24,117916	75,311546	32	F313	20,100754	198,127823	10
V300	23,57486	88,15863	27	V300	19,524551	85,181854	23
D216	22,648029	81,829399	28	L219	17,939308	114,825874	16
K233	22,021591	146,803741	15	T315	16,074234	119,124969	13
Y148	21,444046	163,136398	13	E310	15,227081	185,542252	8
T315	18,124519	76,028595	24	W293	13,988174	173,088669	8
C217	14,44701	73,39473	20	E229	13,955147	113,018036	12
H223	14,288574	157,544525	9	M151	12,332909	133,765137	9
L219	12,85939	86,798889	15	F152	10,711075	142,925064	7
M151	8,160172	159,185501	5	T307	10,20208	100,536865	10
H297	5,93161	128,096268	5	G213	7,645958	60,412914	13
H319	4,82016	110,210571	4	I296	7,538864	142,356735	5
I144	4,725479	102,739929	5	Y299	6,45636	170,339981	4
G213	3,780384	49,322968	8	T220	6,421791	95,373505	7
Y299	3,400726	162,189987	2	F221	4,101685	171,479309	2
F241	0,945099	173,076584	1	S214	4,07901	117,869568	3
S214	0,670212	107,986252	1	A304	3,78038	67,1259	6
F313	0,310654	163,467667	0	H319	1,72821	128,62851	1
				C217	0,931961	89,983391	1

Table S11. Geometric characteristics of the MOR binding site residues within 3.5A of the cyclopeptide **8** (Orientation 1 and 2) after the QM/MM optimization.

Orientation 1				*Orientation 2*			
	Contact (Å^2)	*Exposed (Å^2)*	*%*		*Contact (Å^2)*	*Exposed (Å^2)*	*%*
Binding Site	558,08374	798,133484	70	Binding Site	490,223572	814,875061	60
I322	53,397804	134,600983	40	K303	62,794319	151,818161	41
T218	51,618214	78,402763	66	W318	58,812111	92,46994	64
W318	44,878815	173,075806	26	I322	41,789795	99,398392	42
F221	35,034027	137,313416	26	T218	40,112167	119,982269	33
D216	31,868137	64,77359	49	F237	25,740677	118,512314	22
K303	31,594368	126,491158	25	L219	25,364647	139,461105	18
F237	29,29776	112,625702	26	K233	23,592377	107,182114	22
D147	26,634464	64,235855	41	F221	23,198914	189,182861	12
Y148	25,663498	115,413757	22	I296	22,297211	113,310692	20
W293	22,27533	178,352524	12	W293	21,916306	161,552933	14
K233	21,710236	151,490631	14	V300	16,42572	97,796265	17
C217	21,355644	89,735352	24	D216	15,466911	119,675293	13
V300	20,770214	60,555939	34	E310	13,611069	211,898758	6
T315	13,618599	140,584351	10	M151	11,619179	112,759209	10
F152	10,028488	129,36702	8	T307	9,038086	95,443504	9
H319	9,1007	134,96582	7	Y299	8,505859	158,935349	5
S214	9,07373	81,605133	11	H319	7,700668	96,154243	8
I296	8,177696	126,991577	6	T220	5,946098	88,661774	7
T220	7,135323	95,827232	7	H223	3,141563	118,173172	3
A240	6,897476	78,517464	9	A304	1,890198	65,152245	3
L219	6,239334	119,506363	5	T315	1,420784	87,74015	2
H223	5,666199	148,710907	4	A240	0,237846	58,044582	0
I144	3,78038	101,1362	4	D147	0,237839	147,365311	0
V236	2,205223	128,878036	2				
M151	1,326279	116,724815	1				
G213	0,945099	75,279968	1				
F241	0,630066	161,331985	0				